Gain-assisted superluminal propagation and rotary drag of photon and surface plasmon polaritons

Naveed Khan,[1] Bakht Amin Bacha,[2] Azmat Iqbal,[1,*] Amin Ur Rahman,[1] and A. Afaq[3]
[1]*Department of Physics, The University of Lahore, Punjab, Pakistan*
[2]*Department of Physics, University of Malakand, Chakdara, Dir(L), Pakistan*
[3]*Center of Excellence in Solid State Physics, University of the Punjab, Lahore, Pakistan*
(Received 7 May 2017; published 24 July 2017)

Superluminal propagation of light is a well-established phenomenon and has motivated immense research interest that has led to state-of-the-art knowledge and potential applications in the emerging technology of quantum optics and photonics. This study presents a theoretical analysis of the gain-assisted superluminal light propagation in a four-level N-type atomic system by exploiting the scheme of electromagnetically induced gain and superluminal propagation of surface plasmon polaritons (SPPs) along the gain-assisted atomic-metal interface simultaneously. In addition, a theoretical demonstration is presented on the comparison between Fresnel's rotary photon drag and SPP drag in view of light polarization state rotation by rotating the coherent atomic medium and the atomic-metal interface, respectively. Analogous to photon drag in the superluminal anomalous dispersion region where light polarization rotation occurs opposite the rotation of the gain-assisted atomic medium, the rotation of the atomic-metal interface also rotates the polarization state of SPPs opposite the rotation of the interface. This further confirms the superluminal nature of SPPs propagating along the interface with negative group velocity. Rabi frequencies of the control and pump fields considerably modify both photon and SPP drag coefficients. Metal conductivity also controls SPP propagation.

DOI: 10.1103/PhysRevA.96.013848

I. INTRODUCTION

The advent of innovative laser technology has brought about remarkable revolutions in the fields of quantum optics, photonics, and plasmonics. The application of laser fields on various atomic and solid-state optical media has enabled us to induce and simulate diverse phenomena of fundamental and practical interest such as harmonic generations, four-wave mixing, lasing without inversion, Doppler broadening, electromagnetically induced transparency (EIT), electromagnetically induced gain (EIG), electromagnetically induced absorption (EIA), and so on. Deploying the concept of electromagnetically induced processes to atomic and solid systems, the group index of the medium can be decreased, can be increased, or can even become negative, thus offering huge opportunities for researchers to study superluminal and subluminal light propagation for potential applications. For instance, using the scheme of EIT on a three-level Λ-type atomic system, light can be slowed down owing to quantum interference [1–3]. As such, the opaque atomic medium may become transparent to a probe laser field that couples a lower atomic state to an excited state by the application of a strong controlling laser field that couples another lower state to the same excited state [4]. The exact tuning of the frequency difference of the two fields with that of the two lower-energy states leads to vanishing light absorption, which in turn results in a transparent window in the absorption spectrum. The processes of EIA and EIG leads to peaks and dips, respectively, in the absorption spectrum of probe field [5–7].

Superluminal propagation has been an established research field since the seminal work in the field [8–14]. Nevertheless, the superluminal propagation in the anomalous dispersion region suffers strong light absorption [15] and shape distortion [16] that lead to experimental difficulties and sometimes controversies regarding superluminal propagation interpretations. In fact, in a passive dispersion medium a superluminal light pulse in the anomalous dispersion region experiences enormous loss in intensity [17]. This problem, nevertheless, can be overcome by employing a well-designed active medium that retains transparency in the anomalous dispersion region through intensity amplification via an external energy source. In this regard, Steinberg and Chiao [18] suggested a way out using a gain-assisted medium to study superluminal light propagation in a transparent anomalous dispersion region with negligible pulse distortion. Subsequently, Wang *et al.* [5] and Dogariu *et al.* [6] studied lossless superluminal light propagation in a transparent anomalous dispersion region both experimentally and theoretically by deploying the gain process in a three-level cesium atomic configuration. Recently, Ye *et al.* [19] presented a theoretical and experimental demonstration of superluminal light propagation in a passive Lorentzian medium by creating an anomalous dispersion region away from the absorption peak. Longhi *et al.* [20] and Nimtz *et al.* [21] presented an experimental study of superluminal tunneling of optical pulses across successive potential barriers. Apart from classical and quantum treatments, superluminal propagation has also been studied using a quantum-field-theory approach, especially along undersized waveguides [22,23].

Inspired by the coherent control of light propagation via EIT in various optical media [3,24], researchers have also devoted considerable attention to manipulating light propagation along various interfaces deploying surface plasmon polaritons (SPPs) by quantum coherence. Basically, SPPs are quanta of electromagnetic fields generated by the light coupled to collective electron oscillations moving along the metal-dielectric interface (MDI) [25–27]. Owing to their

*Author to whom correspondence should be addressed: azmatiqbal786@gmail.com

peculiar optical properties, SPPs are considered promising candidates for the emerging technology in the field of quantum optics, photonics, and plasmonics [26,28–36]. As such, the generation, propagation, and decay mechanism of SPPs along the MDI and other surfaces have attracted enormous attention from researchers in recent years. After coupling with conducting electron oscillations, the incident light may propagate along the MDI as confined surface electromagnetic waves. Thus, SPPs may offer subwavelength confinement of light, electric field enhancement, and high correlation to the dielectric constant of the surrounding media [36]. The ability of SPPs to concentrate electromagnetic (EM) fields beyond the diffraction limit makes them suitable for quantum-controlled devices, such as qubit operators, single-photon sources, and transistors [37–39].

The efforts to gain control over large-scale light propagation and its subwavelength confinement by SPPs near the MDI for practical purposes [40,41] have paved the way for the development of theoretical and experimental schemes incorporating a variety of interfaces [42,43]. The SPP-enhanced propagation of electromagnetic energy at the MDI is significantly manipulated by the dielectric constant of metals [44]. However, aside from other dissipative mechanisms absorption at the metal surface, represented by the imaginary part of the SPP wave vector, reduces the propagation length of SPPs. The exponential decay of SPPs normal to the interface renders subwavelength confinement of electromagnetic energy [45]. Attempts to extend the concept of EIT to surface plasmons (SPs) and SPPs offer huge challenges, including Ohmic losses at the interfaces [46] which may defy confinement and long-scale propagation of SPPs. One possible way to overcome such losses is to place a gain-assisted optical medium adjacent to the metal surface. As such, manipulation of light propagation deploying SPPs near gain-assisted media has attracted much interest in recent years [25,47–53]. Aside from compensating the loss, the gain-assisted medium also leads to SPP signal amplification.

Nezhad *et al.* [54] predicted that the presence of the gain-assisted medium reduces the absorption losses in the propagation of SPPs on metal surface. Recently, Jha *et al.* [55] and Dorfman *et al.* [56] presented SPP propagation on a metal surface and in silver nanoparticles, respectively, placed near a gain-assisted medium, exploiting the idea of quantum coherence. More recently, Tan and Huang [57] suggested a scheme of lossless SP propagation deploying four-level N-type quantum emitters at the dielectric-metamaterial interface. They also attained superluminal SP propagation from active Raman gain.

In this paper, we present the superluminal light propagation in a four-level N-type gain-assisted atomic medium by exploiting the scheme of EIG and superluminal SPP propagation by coupling light to collective electronic oscillations along the gain-assisted atomic-metal interface. In addition, we present a theoretical demonstration of the comparison between the celebrated Fresnel rotary photon drag and SPP drag in view of linear polarization state rotation of light by spinning the gain-assisted medium alone and the atomic-metal interface, respectively. The impact of the control field's Rabi frequency, the pump field's detuning and Rabi frequency, and probe detuning on light as well as SPP propagation is explored. The effect of metal conductivity along with specific parameters on SPP propagation and SPP dragging is also investigated. We use a simple yet elegant approach to achieve the aforementioned objectives. The coupling of light to excite collective electronic oscillations on a metal surface as superluminal confined light modes or SPPs propagating along the gain-assisted atomic-metal interface may offer interesting new avenues for researchers regarding fundamental and practical relevance in science. In order to shed light on the dispersion, absorption, and rotary drag of incident light by the gain-assisted medium, we calculate the complex susceptibility of the atomic medium, the corresponding group index, and group velocity. The expressions for the SPP wave vector and group index, which characterize the propagation and dragging features of SPPs along the atomic-metal interface, are also derived in terms of the metal conductivity and permittivity of the atomic and metallic media.

The concept of photon drag dates back to Fresnel, who predicted that light propagating through a moving medium is subject to drag effects [58]. Fresnel's light-drag theory for the longitudinal case was verified experimentally by Fizeau [59]. Later on, Jones [60] presented an experimental demonstration of lateral photon drag in a moving medium using the formula $\Delta x = (n_g - \frac{1}{n_r})\frac{vL}{c}$, where n_r and n_g are the phase and group refractive indices, L is the length of the medium, v is the transverse velocity of a moving medium, and c is the speed of light. Subsequently, rotary photon drag was verified by Jones [61] in a rotating dielectric medium in view of the rotation of the linear polarization state of light through a small angle given as $\theta_r = (n_g - \frac{1}{n_r})\frac{\omega_s L}{c}$, where ω_s is the spin velocity of the medium.

Fresnel drag has attracted enormous attention in recent years because of its fundamental and practical interest. References [62–66] demonstrated light drag by experiments in a slow-light ruby medium. A considerable enhancement in rotary photon drag was observed by Arnold *et al.* [64] in view of light polarization state rotation in a slow-light spinning ruby medium. The linear polarization rotation of light arises from the phase difference between the right- and left-handed circular polarization states which corresponds to the spin angular momentum of light. It is observed that optical spin and orbital angular momentum separately account for the rotation of the polarization state of light and the transmitted image, respectively [67–70].

Light pulses propagating in atomic media with a highly dispersive nature can also experience a dragging effect. Unfortunately, light-drag enhancement in a dispersive atomic medium is often accompanied by strong light absorption at the resonance frequency. However, an experimental demonstration of longitudinal drag in view of the light phase velocity was recently presented by Safari *et al.* [71] for rubidium vapors. At about the same time, Kuan *et al.* [72] observed a further improvement in phase velocity dragging using a three-level cold ^{85}Rb atomic medium with the scheme of EIT. References [71,72] studied only the longitudinal light drag in slow-light media by manipulating the phase velocity of light, in contrast to our theoretical demonstration, which mainly elucidates superluminal rotary photon drag in terms of light group velocity in a gain-assisted atomic medium. Gain-assisted superluminal propagation in a three-level atomic

system was studied in Refs. [5,6] with a different approach. Superluminal light propagation in a gain-assisted four-level N-type atomic medium was studied in Refs. [7,73] with conditions different than ours (e.g., detuning and the number of laser fields). More recently, one of the authors and his collaborators studied rotary photon drag in a four-level cascade-type chiral atomic medium [74] and rotary SPP drag at a four-level tripod atomic-metal interface [75]. In contrast, the current study is mainly concerned with superluminal light propagation under the EIG and rotary photon drag in view of light linear polarization rotation in the four-level N-type gain-assisted nonchiral atomic medium. We also investigate the manifestation of superluminal propagation of SPPs and rotary SPP drag along the four-level N-type gain-assisted atomic-metal interface.

In the sections that follow we discuss the proposed model and its dynamics; the steady-state solution of the optical equation under the dipole and rotating-wave approximation; the numerical results along with a discussion; and a brief summary of the main findings with applications.

II. MODEL AND EQUATIONS OF MOTION

In order to shed light on gain-assisted superluminal light propagation and its rotary drag, we exploit a four-level N-type gain-assisted atomic configuration using the scheme of EIG (Fig. 1). The lower state $|d\rangle$ of the atomic system is coupled with the excited level $|a\rangle$ by a pump field E_1 with Rabi frequency $\Omega_1 = E_1\varrho_{da}/2\hbar$. The lower level $|c\rangle$ is coupled to two upper excited levels, $|a\rangle$ and $|b\rangle$, by the probe and control fields, E_p and E_c, with Rabi frequencies $\Omega_p = E_p\varrho_{ca}/2\hbar$ and $\Omega_c = E_c\varrho_{cb}/2\hbar$, respectively. The quantity ϱ_{ij} represents atomic dipole moments. The detunings of the probe and pump fields are related to the resonance frequencies of the atomic states, i.e., $\Delta_p = \omega_{ac} - \nu_p$ and $\Delta_1 = \omega_{ad} - \nu_1$, where ν_p and ν_1 are the phase velocities of the respective fields. The gain-assisted propagation of SPPs is accomplished by placing the gain-assisted atomic medium near a metal, as shown in Fig. 1. A laser field is coupled to the collective electron oscillations of the metal to generate SPPs on the atomic-metal interface. The SPP propagation along the x axis is supported by the gain medium hosted by the dielectric.

The dynamical equations describing the physical scenario of the problem can be derived from the Hamiltonian $H = H_0 + H_I$ in the dipole and rotating-wave approximation. The self-energy part of the atomic Hamiltonian H_0 is given by

$$H_0 = \hbar\omega_a|a\rangle\langle a| + \hbar\omega_b|b\rangle\langle b| + \hbar\omega_c|c\rangle\langle c| + \hbar\omega_d|d\rangle\langle d|. \quad (1)$$

The Hamiltonian H_I describing atomic interaction with laser fields is then given by

$$H_I = -\frac{\hbar}{2}\Omega_1 e^{-i\Delta_1 t}|d\rangle\langle a| - \frac{\hbar}{2}\Omega_p e^{-i\Delta_p t}|c\rangle\langle a| - \frac{\hbar}{2}\Omega_c|c\rangle\langle b| + \text{H.c.} \quad (2)$$

The general expression of density-matrix elements governing the dynamics of the proposed atomic system is obtained from

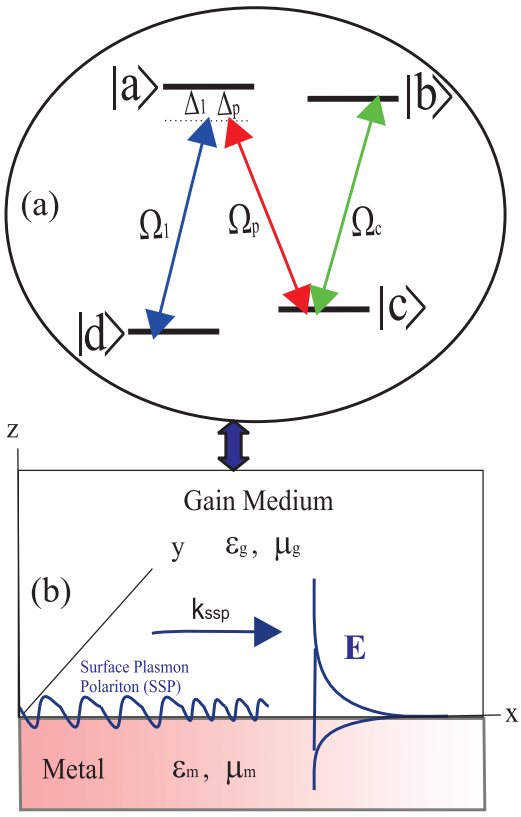

FIG. 1. (a) Schematic of gain-assisted propagation of light in a four-level N-type atomic system under the scheme of electromagnetically induced gain. The gain is accomplished by the probe field of Rabi frequency Ω_p in conjunction with pump and control fields of Rabi frequencies Ω_1 and Ω_c in addition to probe and pump detunings Δ_p and Δ_1, respectively. (b) SPP propagation along an interface between metal and gain-assisted atomic systems (quantum emitters) hosted by a dielectric. The quantum emitters support SPP propagation along the interface. The dielectric medium of permittivity ϵ_d and permeability μ_d occupies the half space $z > 0$, while the metal with permittivity ϵ_m and permeability μ_m is in the half space $z < 0$. As shown, the electric field E of SPPs decays exponentially with respect to distance z from the interface.

the interaction Hamiltonian as follows:

$$\dot{\rho}_{ij} = -\frac{i}{\hbar}[H_I,\rho] - \sum\frac{1}{2}\gamma_{ij}(R^\dagger R\rho + \rho R^\dagger R - 2R\rho R^\dagger), \quad (3)$$

where $R^\dagger$ (R) is the raising (lowering) operator and γ_{ij} represent decay rates of various atomic states.

III. ANALYTICAL RESULTS

By using the dipole and rotating-wave approximation, the time evolution of the density-matrix elements can be conveniently obtained from the master optical equation (3) as in Ref. [73]. In order to understand the implication of EIG in terms of the complex susceptibility χ of the probe field, the steady-state solution for density-matrix elements corresponding to probe transitions can be obtained. Making a second-order expansion to the pump field and a first-order

expansion to the probe field, we can achieve a systematic solution of density-matrix elements [7]. The calculated density-matrix element of states $|a\rangle$ and $|c\rangle$, denoted $\rho_{ac}^{(2)}$, expanded in the second-order pump field and first-order probe field is given by

$$\rho_{ac}^{(2)} = -i\Omega_p\left[\frac{4\Omega_1^2 4\left[(\gamma_{ab}-i\Delta_p)(\gamma_{bd}+\Delta_p-\Delta_1)-i\Omega_c^2\right]}{(-i\gamma_{ad}+\Delta_1)[4(i\gamma_{ab}\Delta_p)(i\gamma_{ac}\Delta_p)-\Omega_c^2]Q} + \frac{8\gamma_{ad}(i\gamma_{ab}+\Delta_p)\Omega_1^2}{(\gamma_{ac}+\gamma_{ad})\left(\gamma_{ad}^2+\Delta_1^2\right)\left(4P+i\Omega_c^2\right)}\right], \tag{4}$$

where $P = (\gamma_{ac}-i\Delta_p)(i\gamma_{ab}+\Delta_p)$ and $Q = 4(i\gamma_{bd}+\Delta_p-\Delta_1)(-i\gamma_{dc}-\Delta_p+\Delta_1)+\Omega_c^2$.

The general formula for the complex susceptibility of the atomic medium is $\chi = 2N|\varrho_{ca}|^2\rho_{ac}/\epsilon_0\hbar\Omega_p$, where N is the density of four-level atoms and ϱ_{ac} is the atomic dipole moment. As the gain is a second-order process [7,73], the calculated susceptibility for the gain-assisted medium obtained from density-matrix elements by keeping all order terms in the control field is as follows:

$$\chi^{(2)} = \frac{3\lambda_0^3}{32\pi^3\epsilon_0\hbar\Omega_p}\rho_{ac}^{(2)}, \tag{5}$$

where λ_0 is the wavelength of incident light.

The real and imaginary parts of the complex susceptibility correspond, respectively, to the probe field dispersion spectrum and gain. The complex dielectric function of the gain-assisted medium is $\epsilon_g = 1+4\pi\chi^{(2)}$. The group index of the probe field in the gain-assisted atomic medium is given by the well-known expression

$$n_g = 1+2\pi\mathrm{Re}[\chi^{(2)}]+2\pi\omega_0\mathrm{Re}\left[\frac{\partial\chi^{(2)}}{\partial\Delta_p}\right], \tag{6}$$

where the medium phase refractive index $n_r = 1+2\pi\mathrm{Re}[\chi]$; therefore, the medium group index in Eq. (6) can be written as $n_g = (n_r+2\pi\omega_0\mathrm{Re}[\frac{\partial\chi^{(2)}}{\partial\Delta_p}])$, from which we can immediately determine the light group velocity as $v_g = c/n_g$.

Being electromagnetic waves bounded by the atomic-metal interface, SPPs are sensitive to the geometry and the nature of the media forming the interface. The propagation features of SPPs at the MDI [42,43] can be well described by the complex wave vector k_{sp}, which is a function of the permittivity of the metallic and dielectric media. Therefore, to characterize the propagation of SPPs along the atomic-metal interface, the passive isotropic dielectric medium is made the host of a gain-assisted atomic medium with complex permittivity $\epsilon_g = \epsilon_g' + i\epsilon_g''$ (with negative ϵ_g'' featuring gain) in the half space $z>0$ and a homogeneous metal surface with complex dielectric function $\epsilon_m = \epsilon_m' + i\epsilon_m''$ in the half space $z<0$ (see Fig. 1). Thus, the SPP propagation is manipulated by the dielectric functions of both the media contained by the wave vector, which can be obtained by applying Maxwell's equations for a transverse-magnetic (TM) field mode [55] with the continuity condition on the interface ($z=0$). The resulting SPP wave vector is written as

$$k_{sp} = \frac{2\pi}{\lambda_0}\sqrt{\frac{\epsilon_g\epsilon_m}{\epsilon_g+\epsilon_m}}. \tag{7}$$

By definition $k_{sp} = k_{sp}^r + ik_{sp}^i = k_0 n_r^{sp}$. Here, $k_0 = 2\pi/\lambda_o$ is the wave vector of incident radiation in free space, and n_r^{sp} is the refractive index of SPPs along the atomic-metal interface, given by

$$n_r^{sp} = \sqrt{\frac{\epsilon_g e_m}{\epsilon_g+e_m}}. \tag{8}$$

The refractive index n_m of the conducting medium in the presence of the probe field is given as $n_m = k_m/k_o$, where k_m is the wave vector of the probe field propagating in the conducting medium and is given by [76]

$$k_m^2 = \mu_m\epsilon_m(\omega_o+\Delta_p)^2 + i\mu_m\sigma(\omega_o+\Delta_p), \tag{9}$$

where $\omega = \omega_0+\Delta_p$ is the atomic resonance frequency, ω_o is the probe field's angular frequency, and Δ_p is the probe field's detuning. Here, ϵ_0 and μ_0 are the permittivity and permeability of free space, and ϵ_m and μ_m are those for metal, while σ is the metal conductivity. For metal, the expressions for complex conductivity, permittivity, and permeability are, respectively, $\sigma = |\sigma|e^{i\phi_1}$, $\epsilon_m = \epsilon_o\epsilon_r^m$, and $\mu_m = \mu_o\mu_r^m$, while the relative permittivity and permeability of metal are, respectively, $\epsilon_r^m = |\epsilon_r^m|e^{i\phi_2}$ and $\mu_r^m = |\mu_r^m|e^{i\phi_3}$. We further assume that the real part of the metal permittivity $\epsilon_m' < 0$ and its absolute value is larger than other components of permittivity, namely, ϵ_m', ϵ_g', and ϵ_g''.

Macroscopically, the refractive index of the conducting medium in terms of its permittivity is $n_m = \sqrt{\epsilon_m}$; therefore, in our case of the gain-assisted medium, the wave vector k_{sp} [Eq. (8)] in terms of the refractive index of metal n_m is given by

$$k_{sp} = \frac{2\pi}{\lambda_o}\sqrt{\frac{\epsilon_g n_m^2}{\epsilon_g+n_m^2}}. \tag{10}$$

The intensity of the SPP field along the metal surface decreases exponentially with the propagation length L as $e^{-2k_{sp}L}$ (Fig. 1). The propagation length of SPPs is the distance traveled by SPPs along the metal for which intensity reduces to $1/e$ of its original value. The propagation length of SPPs [43] is given by the imaginary part of the SPP wave vector as $L = 1/2k_{sp}^i$.

Thus, propagation of SPPs depends considerably on the dielectric constant of the metal surface, relative permittivity of the two media, and wavelength of incident light. Now the SPP group index analogous to Eq.(6) can be written in terms of n_r^{sp} as

$$n_g^{sp} = n_r^{sp} + \omega_0\mathrm{Re}\left[\frac{\partial n_r^{sp}}{\partial\Delta_p}\right]. \tag{11}$$

Therefore, the group velocity of SPPs is $v_g^{sp} = c/n_g^{sp}$.

Now the rotary photon drag [61] for the probe and SPP mode is described by the relation

$$\left(\theta_r,\theta_r^{sp}\right) = \left(n_g,n_g^{sp}-\frac{1}{n_r,n_r^{sp}}\right)\frac{\omega_s L}{c}. \tag{12}$$

The respective rotary photon drag can be determined by plugging Eqs. (6) and (11) into Eq. (12).

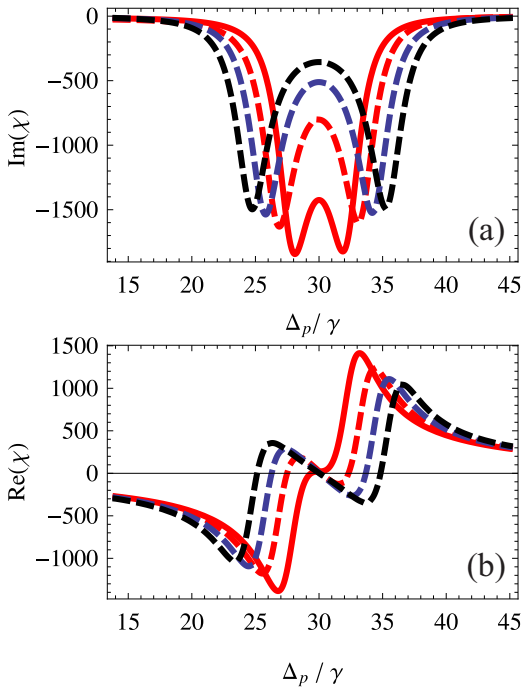

FIG. 2. Variation of (a) the imaginary and (b) real parts of χ with probe detuning for fixed control field values $\Omega_c = 5\gamma$ (solid red line), 7γ (dashed red line), 9γ (dashed blue line), 11γ (dashed black line) with the parameters $\gamma_{ac,ad,bd} = 2.5\gamma$, $\gamma_{ab,cd} = 0.5\gamma$, $\Delta_1 = 30\gamma$, $\Omega_1 = 2.5\gamma$, $\omega_o = 10^3\gamma$.

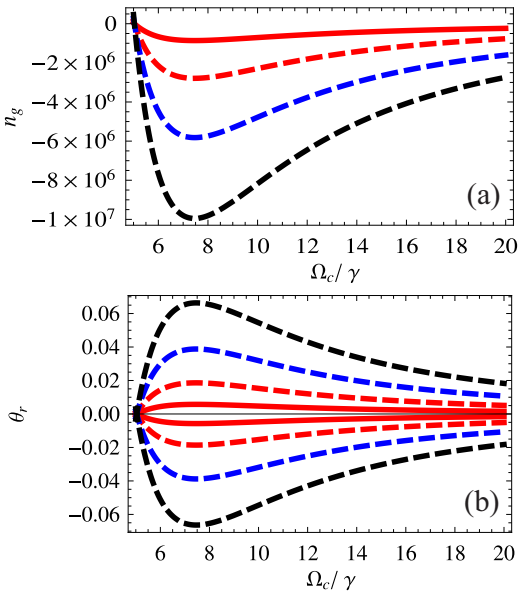

FIG. 3. Variation in the group index and rotary photon drag with the control field's Rabi frequency Ω_c with the parameters $\gamma_{ac,ad,bd} = 2.5\gamma$, $\gamma_{ab,cd} = 0.5\gamma$, $\omega_0 = 10^3\gamma$, $L = 10$ cm, $\omega_s = \pm 20$ rps, $\Omega_1 = 2.5\gamma$ (solid red line), $\Omega_1 = 4.5\gamma$ (dashed red line), $\Omega_1 = 6.5\gamma$ (dashed blue line), $\Omega_1 = 8.5\gamma$ (dashed black line).

IV. NUMERICAL RESULTS AND DISCUSSION

The group velocity of a light pulse depends upon the nature of slope of the dispersion spectrum [plot of Re(χ) versus the probe field detuning]. In general, the positive slope of the dispersion spectrum corresponds to subluminal light propagation, while its negative slope describes superluminal light propagation. Also, Im(χ) > 0 implies probe field gain, while Im(χ) < 0 implies probe field absorption.

Figure 2 displays the features of complex susceptibility of a stationary gain-assisted medium with probe field detuning Δ_p. As shown, the susceptibility of the gain-assisted medium depends considerably on Δ_p as well as control field Rabbi frequency Ω_c at fixed pump Rabi frequency $\Omega_1 = 2.5\gamma$ and pump detuning $\Delta_1 = 30\gamma$. The gain character of the medium [Im(χ) < 0] is revealed by the imaginary part of the susceptibility [Fig. 2(a)], while its real part [Fig. 2(b)] shows the dispersive behavior of the medium to the probe field. The solid red line corresponds to $\Omega_c = 5\gamma$. The gain doublet occurs in the imaginary part around $\Delta_p = 30\gamma$ when the control field is tuned with the $|b\rangle \leftrightarrow |c\rangle$ transition resonance. The two gain dips at the resonant control field correspond to the superposition of dressed states $|b\rangle$ and $|c\rangle$ as $|\pm\rangle = (|b\rangle \pm |c\rangle)/\sqrt{2}$ [7]. The gain doublet is further manipulated with the control field of Rabbi frequencies 7γ, 9γ, and 11γ. The width of the gain doublet increases with the strength of the control field.

Figure 3 elucidates the dependence of the group index n_g [Fig. 3(a)] and rotary photon drag θ_r [Fig. 3(b)] on the control field Rabi frequency Ω_c for various values of the pump field Rabi frequency: $\Omega_1 = 2.5\gamma$ (solid red curve), $\Omega_1 = 4.5\gamma$ (dashed red curve), $\Omega_1 = 6.5\gamma$ (dashed blue curve), and $\Omega_1 = 8.5\gamma$ (dashed black curve). The fixed parameters are decay rates $\gamma_{ac,ad,bd} = 2.5\gamma$ and $\gamma_{ab,cd} = 0.5\gamma$, the probe field resonance frequency $\omega_0 = 10^3\gamma$, the length of the atomic ensemble $L = 10$ cm, and medium spin angular frequency $\omega_s = \pm 20$ rps. Negative n_g in the anomalous dispersive region implies the superluminal feature of light propagation [Fig. 3(a)]. As shown, n_g first decreases and then increases with Ω_c to attain a saturation value for fixed Ω_1 changing stepwise from 2.5γ to 8.5γ. The maximum (negative) value of n_g equals $\sim 10^7$, which corresponds to a drag coefficient of 0.066 rad. Furthermore, n_g increases with pump field Rabi frequency Ω_1. Figure 3(b) shows the rotary photon drag dependence on Ω_c in view of probe field polarization state rotation at fixed spin angular frequency of the atomic medium ω_s. For negative (positive) ω_s, the positive (negative) values of θ_r at $\Omega_1 = 2.5\gamma, 4.5\gamma, 6.5\gamma, 8.5\gamma$ are shown, respectively, by the solid red, dotted red, black, and blue lines, which indicate that photon drag takes place opposite the medium rotation. This in turn is consistent with earlier studies implying superluminal light propagation.

Figure 4 describes variation in θ_r with respect to ω_s for the same parameters as in Fig. 3. As shown, the rotary photon drag coefficient θ_r increases with ω_s. However, the light dragging takes place opposite the rotation of the medium; that is, if rotation is clockwise, the dragging will be anticlockwise and vice versa (as shown with opposite signs of θ_r and ω_s). The maximum value of photon drag is $\sim \mp 0.032$ rad at $\omega_s = \pm 20$ rps.

Figure 5 encapsulates variation in the real and imaginary parts of SPP wave vector k_{sp} with the Rabi frequency of control field Ω_c at various values of Δ_p while other parameters are

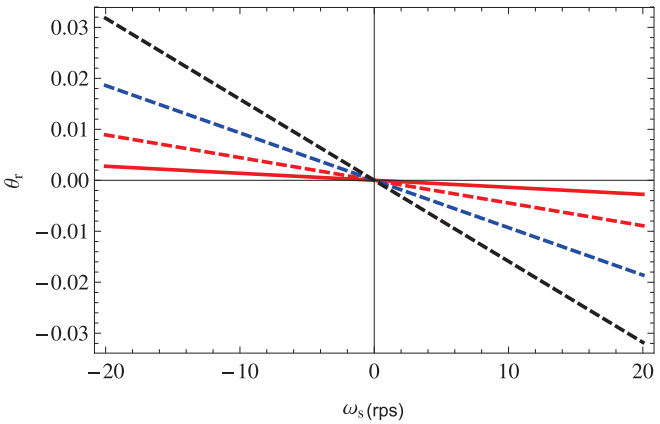

FIG. 4. Dependence of photon drag on rotation speed of the gain-assisted atomic medium with the spectral parameters $\gamma_{ac,ad,bd} = 2.5\gamma, \gamma_{ab,cd} = 0.5\gamma, \omega_0 = 10^3\gamma, L = 10\,\text{cm}, \Omega_3 = 5.5\gamma, \Delta_1 = 30\gamma$, $\Omega_1 = 2.5\gamma$ (solid red line), $\Omega_1 = 4.5\gamma$ (dashed red line), $\Omega_1 = 6.5\gamma$ (dashed blue line), $\Omega_1 = 8.5\gamma$ (dashed black line).

fixed (e.g., decay rates, pump field, permittivity and permeability of the media, phase angles, and metal conductivity). The imaginary part of k_{sp} [Fig. 5(a)] represents SPP absorption, while its real part [Fig. 5(b)] corresponds to the dispersion spectrum. The absorption increases by increasing Ω_c (from 0γ to 20γ). The top solid red absorption line at detuning $\Delta_p = 30\gamma$ corresponds to the central peak between the gain doublets in Fig. 2(a). The two pairs of closely spaced dashed lines (red and green) below the solid red line in the absorption spectrum correspond to the gain doublet at probe detunings: $(28\gamma,32\gamma)$ and $(27\gamma,33\gamma)$, respectively. The corresponding

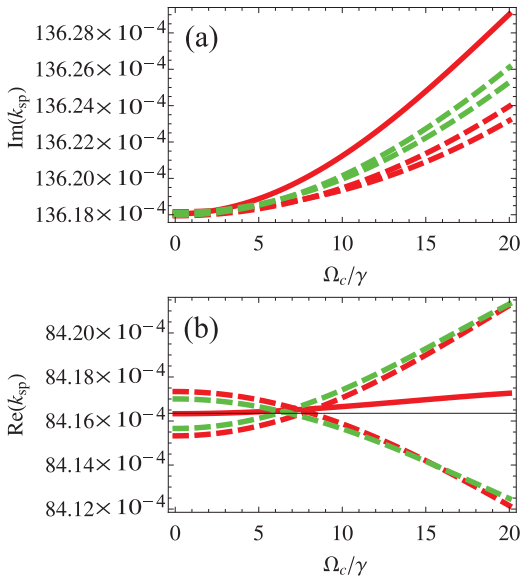

FIG. 5. Variation of (a) the imaginary part and (b) the real part of wave vector k_{sp} for SPPs with Ω_c/γ at fixed parameters: $\gamma_{ac,ad,bd} = 2.5\gamma, \gamma_{ab,cd} = 0.5\gamma, \Omega_1 = 2.5\gamma, \mu_0(\mu_m) = 1, (\epsilon_0)\epsilon_m = 1, \Delta_p = 30\gamma$ (solid red line), $\Delta_p = (27,33)\gamma$ (dashed red line), $\Delta_p = (28,32)\gamma$ (dashed green line), $\varphi_{1,2,3} = \pi/2$, $|\sigma| = 2$ S/m.

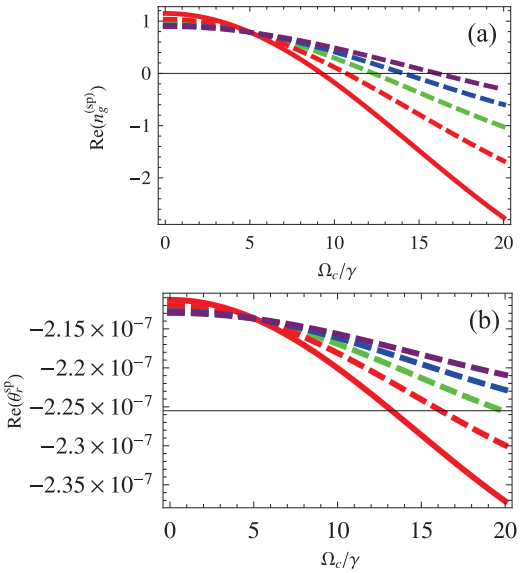

FIG. 6. Impact of Ω_c/γ on group index and the rotary SPP drag with the parameters $\gamma_{ac,ad,bd} = 2.5\gamma$, $\gamma_{ab,cd} = 0.5\gamma$, $\mu_0(\mu_m) = 1$, $(\epsilon_0)\epsilon_m = 1$, $\omega_s = 20$ rps, $\Delta_{1,p} = 30\gamma$, $\varphi_{1,2,3} = \pi/2$, $|\sigma| = 2$ S/m, $\omega_0 = 10^3\gamma$, $\Omega_1 = 2.5\gamma$ (solid red line), $\Omega_1 = 3\gamma$ (dashed red line), $\Omega_1 = 3.5\gamma$ (dashed green line), $\Omega_1 = 4\gamma$ (dashed blue line), $\Omega_1 = 4.5\gamma$ (dashed purple line).

pairs of dispersion lines are shown in Fig. 5(b). As shown, at any value of Δ_p the dispersion is less than 1 [Re(k_{sp}) < 1], thus implying superluminal SPP propagation at the interface of the gain-assisted medium and metal.

Figures 6(a) and 6(b) demonstrate the effect of Ω_c on the SPP group index n_g^{sp} [Eq. (11)] and rotary SPP drag θ_r^{sp} [Eq. (12)] for various values of pump field Rabbi frequency Ω_1 at fixed Δ_p, Δ_1, σ, and ω_s. Figure 6(a) clearly explicates a noticeable decrease in n_g^{sp} by increasing Ω_c for any fixed value of Ω_1. However, an increase in Ω_1 causes a noticeable increase in n_g^{sp}. The maximum negative value of n_g^{sp} ($\sim$3) found at $\Omega_1 = 2.5\gamma$ shown by the solid red curve [Fig. 6(a)] corresponds to the negative drag coefficient θ_r^{sp} of SPPs with a value of $\sim 2.37 \times 10^{-7}$ rad [Fig. 6(b)]. The rotary SPP drag increases with an increase in Ω_c at a particular value of Ω_1, which is due to the corresponding change in the group index in Fig. 6(a). The negative SPP drag implies that analogous to photon drag, SPP polarization state rotation also takes place opposite the rotation of the atomic-metal interface, which implies superluminal SPP propagation.

Figure 7 explicates the variation of n_g^{sp} and θ_r^{sp} in the gain doublet region with Ω_c for various values of Δ_p while other parameters are fixed as in Fig. 6. The variation trend is identical to that in Fig. 6. From Fig. 7(a) it is noted that for various values of probe detuning $(27\gamma, 30\gamma, 32\gamma, 33\gamma)$, a noticeable decrease in n_g^{sp} occurs by increasing Ω_c except for the counterchange at $\Delta_p = 28\gamma$ (top dashed curve). Figure 7(b) shows that θ_r^{sp} increases by increasing Ω_c at a fixed Δ_p, except for the counterchange at $\Delta_p = 28\gamma$.

Figure 8 elucidates SPP drag θ_r^{sp} as a function of the spin angular velocity ω_s of the atomic-metal interface for various values of metal conductivity. As shown, analogous to the rotary photon drag in the superluminal region taking place

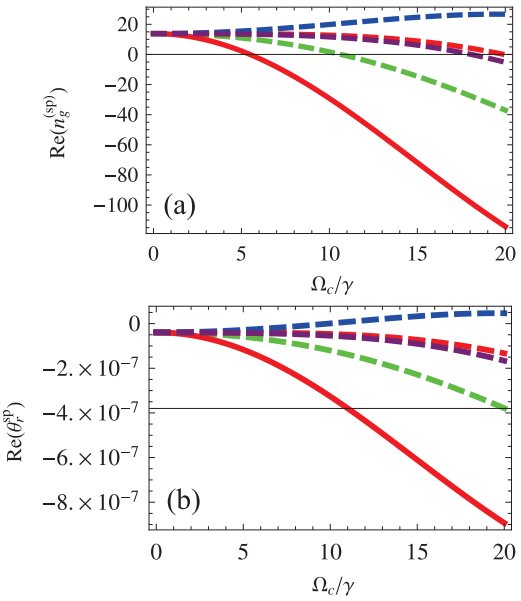

FIG. 7. Variation in the group index and rotary SPP drag with Ω_c/γ with the parameters $\gamma_{ac,ad,bd} = 2.5\gamma$, $\gamma_{ab,cd} = 0.5\gamma$, $\mu_0(\mu_m) = 1$, $(\epsilon_0)\epsilon_m = 1$, $\Delta_1 = 30\gamma$, $\omega_s = 20$ rps, $\varphi_{1,2,3} = \pi/2$, $|\sigma| = 10$ S/m, $\omega_0 = 10^3\gamma$, $\Omega_1 = 2.5\gamma$, $\Delta_p = 30\gamma$ (solid red line), $\Delta_p = 27\gamma$ (dashed red line), $\Delta_p = 28\gamma$ (dashed green line), $\Delta_p = 33\gamma$ (dashed blue line), $\Delta_p = 32\gamma$ (dashed purple line).

opposite the rotation of the atomic medium (Fig. 4), the SPP drag also takes place opposite the rotation of the atomic-metal interface. This further confirms SPP superluminal propagation and indicates that in the superluminal region if the medium is subject to rotating in the clockwise direction, then the SPP drag takes place in the counterclockwise direction and vice versa. Furthermore, the SPP drag has an inverse relation with the metal conductivity. The increase in the value of the conductivity from $|\sigma| = 10$ S/m (dashed green line) to $|\sigma| = 50$ S/m (dashed purple line) results in a decrease in the SPP drag coefficient. The SPP drag coefficient has a maximum value of $\mp 1.2 \times 10^{-7}$ rad for $\omega_s = \pm 20$ when $|\sigma| = 10$ S/m and a minimum value of 0 rad for $\omega_s = \pm 20$ when $|\sigma| = 50$ S/m for metal conductivity while keeping other parameters constant. The change in conductivity may change the plasmon frequency of collective electronic oscillations, which may result in the corresponding change in the refractive index and hence SPP drag.

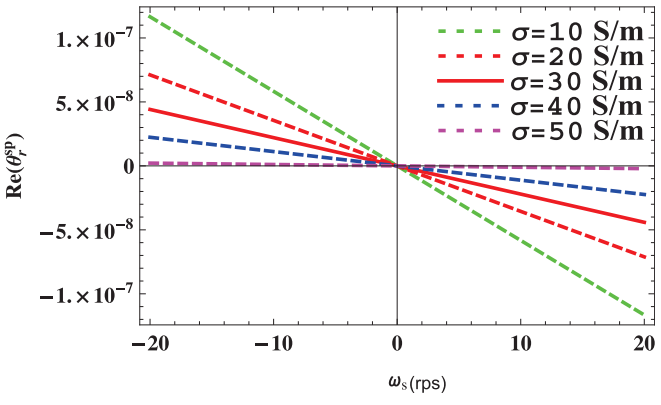

FIG. 8. Dependence of SPP drag on the rotation velocity of the atomic-metal interface and metal conductivity such that $\gamma_{ac,ad,bd} = 2.5\gamma$, $\gamma_{ab,cd} = 0.5\gamma$, $\mu_0(\mu_m) = 1$, $(\epsilon_0)\epsilon_m = 1$, $\Delta_1 = 30\gamma$, $\varphi_{1,2,3} = \pi/2$, $\omega_0 = 10^3\gamma$, $\Omega_1 = 2.5\gamma$, $\Delta_p = 30\gamma$, $\Omega_c = 5\gamma$, $|\sigma| = 10$ S/m (dashed green line), $|\sigma| = 20$ S/m (dashed red line), $|\sigma| = 30$ S/m (solid red line), $|\sigma| = 40$ S/m (dashed blue line), $|\sigma| = 50$ S/m (dashed purple line).

V. CONCLUSION

To sum up, we have presented a theoretical analysis of superluminal light propagation in a four-level N-type gain-assisted atomic medium using the EIG coherency and superluminal SPP propagation along the gain-assisted atomic-metal interface. In addition, a comparative investigation between rotary photon drag and SPP drag has been carried out using this scheme. We observed a prominent gain doublet in the anomalous dispersion spectrum of the probe field [Fig. 2(a)]. The maximum negative group index of the probe light is $\sim 10^7$ [Fig. 3(a)], which manifests superluminal light propagation in the gain-doublet region with a negative group velocity with a magnitude of 30 m/s. The corresponding observed photon drag coefficient θ_r representing photon polarization state rotation has a magnitude of 0.066 rad [Fig. 3(b)], while the maximum value of photon drag is $\sim \mp 0.032$ rad at $\omega_s = \pm 20$ rps (Fig. 4). When light is coupled to electronic oscillations of metal placed near a gain-assisted atomic medium, superluminal light modes in the form of SPPs are generated and propagate along the atomic-metal interface with a maximum negative group index of 115 [Fig. 7(a)] with a negative group velocity of $\sim 2.6 \times 10^6$ m/s. The maximum negative drag coefficient of SPPs predicted by the model is $\sim 9 \times 10^{-7}$ rad [Fig. 7(b)] at $\Omega_c/\gamma = 20$. However, the maximum SPP drag coefficient has a value of $\mp 1.2 \times 10^{-7}$ rad for $\omega_s = \pm 20$ at the lowest metal conductivity, $|\sigma| = 10$ S/m, while it is zero at the highest metal conductivity, $|\sigma| = 50$ S/m (Fig. 8) while keeping other parameters constant. With the proposed theoretical model, we have simultaneously studied the superluminal features of both light and SPPs in an anomalous dispersion region, and the associated light-drag coefficients have been measured. Control of the superluminal propagation of light and SPPs as well as drag coefficients has been accomplished either by changing the spinning velocity of the host medium or by changing the control field's Rabi frequency by keeping other parameters constant. Analogous to photon drag in the superluminal anomalous dispersion region, where light polarization rotation occurs opposite the rotation of the gain-assisted atomic medium, the rotation of the atomic-metal interface also rotates the polarization state of SPPs opposite the rotation of the interface. This further confirms superluminal features of SPPs propagating with superluminal group velocity. The conductivity of the metal and probe detuning also influence the SPP propagation to a considerable extent. The predictions of the proposed model may be of considerable interest for potential applications in the fields of quantum optics, photonics, and plasmonics.

[1] O. A. Kocharovskaya and Ya. I. Khanin, Sov. Phys. JETP **63**, 945 (1986).
[2] K. J. Boller, A. Imamoglu, and S. E. Harris, Phys. Rev. Lett. **66**, 2593 (1991).
[3] S. E. Harris, Phys. Today **50**(7), 36 (1997).
[4] M. D. Lukin and A. Imamoglu, Nature (London) **413**, 273 (2001).
[5] L. J. Wang, A. Kuzmich, and A. Dogariu, Nature (London) **406**, 277 (2000).
[6] A. Dogariu, A. Kuzmich, and L. J. Wang, Phys. Rev. A **63**, 053806 (2001).
[7] G. S. Agarwal and S. Dasgupta, Phys. Rev. A **70**, 023802 (2004).
[8] L. Rayleigh, Nature (London) **24**, 382 (1881).
[9] L. Rayleigh, Philos. Mag. **48**, 151 (1899).
[10] L. Brillouin, *Wave Propagation and Group Velocity* (Academic, New York, 1960).
[11] M. Born and E. Wolf, *Principles of Optics*, 7th ed. (Cambridge University Press, Cambridge, 1997).
[12] L. D. Landau and E. Lifshitz, *Electrodynamics of Continuous Media* (Pergamon, Oxford, 1960), p. 286.
[13] C.-G. Huang and Y.-Z. Zhang, Phys. Rev. A **65**, 015802 (2001).
[14] H. Cao, A. Dogariu, and L. J. Wang, IEEE J. Sel. Top. Quantum Electron. **9**, 52 (2003).
[15] S. Chu and S. Wong, Phys. Rev. Lett. **48**, 738 (1982).
[16] B. Segard and B. Macke, Phys. Lett. A **109**, 213 (1985).
[17] W. Withayachumnankul, B. M. Fischer, B. Ferguson, B. R. Davis, and D. Abbott, Proc. IEEE **98**, 1775 (2010).
[18] A. M. Steinberg and R. Y. Chiao, Phys. Rev. A **49**, 2071 (1994).
[19] D. Ye, G. Zheng, J. Wang, Z. Wang, S. Qiao, J. Huangfu, and L. Ran, Sci. Rep. **3**, 1628 (2013).
[20] S. Longhi, P. Laporta, M. Belmonte, and E. Recami, Phys. Rev. E **65**, 046610 (2002).
[21] G. Nimtz, A. Haibel, and R.-M. Vetter, Phys. Rev. E **66**, 037602 (2002).
[22] Z.-Y. Wang, C.-D. Xiong, and B. He, Phys. Rev. A **75**, 013813 (2007).
[23] Z. Y. Wang and C. D. Xiong, Phys. Rev. A **75**, 042105 (2007).
[24] M. O. Scully and M. S. Zubairy, *Qunatum Optics* (Cambridge University Press, Cambridge, 1997).
[25] H. Ditlbacher, J. R. Krenn, G. Schider, A. Leitner, and F. R. Aussenegg, Appl. Phys. Lett. **81**, 1762 (2002).
[26] W. L. Barnes, A. Dereux, and T. W. Ebbesen, Nature (London) **424**, 824 (2003).
[27] M. Bernardi, J. Mustafa, J. B. Neaton, and S. G. Louie, Nat. Commun. **6**, 7044 (2015).
[28] Z. Zhang, Y. Fang, W. Wang, L. Chen, and M. Sun, Adv. Sci. **3**, 1500215 (2016).
[29] M. S. Tame, K. R. McEnery, S. K. Özdemir, J. Lee, S. A. Maier, and M. S. Kim, Nat. Phys. **9**, 329 (2013).
[30] J. M. Fitzgerald, P. Narang, R. V. Craster, S. A. Maier, and V. Giannini, Proc. IEEE **104**, 2307 (2016).
[31] T. W. Ebbesen, H. J. Lezec, H. F. Ghaemi, T. Thio, and P. A. Wolff, Nature (London) **391**, 667 (1998).
[32] J. B. Pendry, Phys. Rev. Lett. **85**, 3966 (2000).
[33] E. Ozbay, Science **311**, 189 (2006).
[34] M. I. Stockman, Nano Lett. **6**, 2604 (2006).
[35] R. Kolesov, B. Grotz, G. Balasubramanian, R. J. Stöhr, A. A. L. Nicolet, P. R. Hemmer, F. Jelezko, and J. Wrachtrup, Nat. Phys. **5**, 470 (2009).
[36] X. Wang, Y. Deng, Q. Li, Y. Huang, Z. Gong, K. B. Tom, and J. Yao, Light Sci. Appl. **5**, e16179 (2016).
[37] E. Altewischer, M. P. van Exter, and J. P. Woerdman, Nature (London) **418**, 304 (2002).
[38] A. V. Akimov, A. Mukherjee, C. L. Yu, D. E. Chang, A. S. Zibrov, P. R. Hemmer, H. Park, and M. D. Lukin, Nature (London) **450**, 402 (2007).
[39] S. Kumar, A. Huck, and U. L. Andersen, Nano Lett. **13**, 1221 (2013).
[40] S. A. Maier, *Plasmonics: Fundamentals and Applications* (Springer, New York, 2007).
[41] D. K. Gramotnev and S. I. Bozhevolnyi, Nat. Photonics **4**, 83 (2010).
[42] J. M. Pitarke, V. M. Silkin, E. V. Chulkov, and P. M. Echenique, Rep. Prog. Phys. **70**, 1 (2007).
[43] J. Zhang, L. Zhang, and W. Xu, J. Phys. D. **45**, 113001 (2012).
[44] A. K. Azad, Y. Zhao, W. Zhang, and M. He, Opt. Lett. **31**, 2637 (2006).
[45] L. O. Diniz, F. D. Nunes, E. Marega, Jr., and B. H. V. Borges, Appl. Phys. A **103**, 649 (2011).
[46] V. M. Agranovich and D. L. Mills, *Surface Polaritons: Electromagnetic Waves at Surfaces and Interfaces* (North-Holland, Amsterdam, 1982).
[47] D. J. Bergman and M. I. Stockman, Phys. Rev. Lett. **90**, 027402 (2003).
[48] J. Seidel, S. Grafström, and L. Eng, Phys. Rev. Lett. **94**, 177401 (2005).
[49] M. A. Noginov, G. Zhu, A. M. Belgrave, R. Bakker, V. M. Shalaev, E. E. Narimanov, S. Stout, E. Herz, T. Suteewong, and U. Wiesner, Nature (London) **460**, 1110 (2009).
[50] R. F. Oulton, V. J. Sorger, T. Zentgraf, R. M. Ma, C. Gladden, L. Dai, G. Bartal, and X. Zhang, Nature (London) **461**, 629 (2009).
[51] O. Hess, J. B. Pendry, S. A. Maier, R. F. Oulton, J. M. Hamm, and K. L. Tsakmakidis, Nat. Mater. **11**, 573 (2012).
[52] J. Grandidier, G. Francs, S. Massenot, A. Bouhelier, L. Markey, J. C. Weeber, C. Finot, and A. Dereux, Nano Lett. **9**, 2935 (2009).
[53] O. Hess and K. L. Tsakmakidis, Science **339**, 654 (2013).
[54] M. P. Nezhad, K. Tetz, and Y. Fainman, Opt. Express **12**, 4072 (2004).
[55] P. K. Jha, X. Yin, and X. Zhang, Appl. Phys. Lett. **102**, 091111 (2013).
[56] K. E. Dorfman, P. K. Jha, D. V. Voronine, P. Genevet, F. Capasso, and M. O. Scully, Phys. Rev. Lett. **111**, 043601 (2013).
[57] C. Tan and G. Huang, Phys. Rev. A **91**, 023803 (2015).
[58] A. J. Fresnel, Ann. Chim. Phys. **9**, 57 (1818); C. C. Adams, *The Knot Book: An Elementary Introduction to the Mathematical Theory of Knots* (American Mathematical Society, Providence, RI, 2004).
[59] A. H. L. Fizeau, C. R. Hebd. Seances Acad. Sci. **33**, 349 (1851); H. Kauffman, *Knots and Physics*, 3rd ed. (World Scientific, Singapore, 2000).
[60] R. V. Jones, Proc. R. Soc. London, Ser. A. **328**, 337 (1972).
[61] R. V. Jones, Proc. R. Soc. London, Ser. A **345**, 351 (1975).
[62] M. Padgett, G. Whyte, J. Girkin, A. Wright, L. Allen, P. Ohberg, and S. M. Barnett, Opt. Lett. **31**, 2205 (2006).
[63] J. Leach, A. J. Wright, J. B. Gotte, J. M. Girkin, L. Allen, S. Franke-Arnold, S. M. Barnett, and M. J. Padgett, Phys. Rev. Lett. **100**, 153902 (2008).

[64] S. F. Arnold, G. Gibson, R. W. Boyd, and M. J. Padgett, Science **333**, 65 (2011).
[65] E. Wisniewski-Barker, G. M. Gibson, S. Franke-Arnold, Z. Shi, P. Narum, R. W. Boyd, and M. J. Padgett, New J. Phys. **16**, 123054 (2014).
[66] E. Wisniewski-Barker, G. Gibson, S. Franke-Arnold, Z. Shi, P. Narum, R. W. Boyd, and M. J. Padgett, Proc. SPIE **9378**, 93780D (2015).
[67] L. Allen, M. W. Beijersbergen, R. J. C. Spreeuw, and J. P. Woerdman, Phys. Rev. A **45**, 8185 (1992).
[68] L. Allen, M. Babiker, and W. L. Power, Opt. Commun. **112**, 141 (1994).
[69] L. Allen, M. J. Padgett, and M. Babiker, Prog. Opt. **39**, 291 (1999).
[70] J. B. Gotte, S. M. Barnett, and M. Padgett, Proc. R. Soc. London, Ser. A **463**, 2185 (2007).
[71] A. Safari, I. D. Leon, M. Mirhosseini, O. S. Magaña-Loaiza, and R. W. Boyd, Phys. Rev. Lett. **116**, 013601 (2016).
[72] P.-C. Kuan, C. Huang, W. S. Chan, S. Kosen, and S.-Y. Lan, Nat. Commun. **7**, 13030 (2016).
[73] B. A. Bacha, I. Ahmad, A. Ullah, and H. Ali, Phys. Scr. **88**, 045402 (2013).
[74] A. A. Khan, B. A. Bacha, and R. A. Khan, Phys. Lett. A **380**, 3724 (2016).
[75] A. Ali, B. A. Bacha, M. S. A. Jabar, A. A. Khan, R. Uddin, and I. Ahmad, Laser Phys. **26**, 095204 (2016).
[76] J. Weiner and F. D. Nunes, Opt. Express **16**, 21256 (2008).